JOURNAL OF MATERIALS SCIENCE 13 (1978) 2164–2170

The mechanical behaviour of cuprous oxide

G. TORRES–VILLASEÑOR, R. BARRIO–PAREDES
Centro de Investigación de Materiales, Universidad Nacional Autónoma de México, Apartado Postal 70-360, México 20

S. VICTOR RADCLIFFE
Divison of Metallurgy and Materials Science, Case Western Reserve University, Cleveland, Ohio 44106, USA

The stress–strain behaviour under compresion at constant strain rate of single crystals (⟨0 5 1⟩ and ⟨1 2 2⟩ compression axis) and polycrystalline samples of cuprous oxide have been examined at room temperature and hydrostatic pressure up to 12 kb and at atmospheric pressure and high temperature up to 600° C. At high environmental pressure, plastic flow occurs at 6 kb. At high temperatures and one atmosphere, extensive plastic deformation was observed after 500° C. The resultant slip planes were of the {1 1 0} and {1 0 0} types. Transmission electron microscopy of thin foils prepared from deformed specimens shows that the Burgers' vectors of the glide dislocations are of the ⟨1 1 1⟩, ⟨1 1 0⟩ and ⟨1 0 0⟩ types.

1. Introduction

Cuprous oxide has a unique type of crystal structure. A simple way of looking at the structure is to consider the oxygen ions as ordered on a b c c lattice with the copper ions occupying the sites of a f c c lattice [1]. The structure may be considered as two completely interpenetrating and identical frameworks [2] of the anti-β-cristobalite type which are not cross-connected by primary Cu–O bonds. It is a structure of 4:2 coordination; each oxygen atom is surrounded by four copper atoms arranged at the corners of a tetrahedron and each copper atom is adjacent to two oxygen atoms. According to Swanson and Fugat [3] the unit cell parameter "a" of Cu_2O is 4.2692 Å, the value listed in the ASTM data file.

Tylecote [4] in 1950 studied the tensile properties of filaments formed by oxidizing copper wire and showed that, although brittle at room temperature, as much as 12% elongation occurred at 500 and 600° C and 25% at 700° C. Vagnard and Washburn [1] extended these observations to compressive stress–strain measurements (constant strain rate) made in the range from room temperature to 600° C on randomly oriented single crystals and polycrystalline Cu_2O prepared by the method of Toth *et al.* [5]. The operative glide plane {0 1 0} was identified in [1] by observing slip traces on two randomly oriented perpendicular surfaces of deformed single crystals. The operative glide direction was identified as ⟨1 0 0⟩ by electron microscopy techniques.

Recently M. Martínez Clemente [6] in accordance with the results of G. Torres Villaseñor [7] found that the {1 1 0} plane is another active plane in Cu_2O.

In the light of these previous studies, the present investigation has been directed first to establishing whether fracture in mechanical tests at room temperature in Cu_2O can be inhibited by increasing the environmental pressure, and if so, to identify the nature of the resulting plastic slip processes. Some high temperature and atmospheric pressure deformation experiments were performed in order to compare the slip behaviour at high temperature with that observed at high pressures and room temperatures.

2. Experimental materials and procedures

2.1. Specimen preparation

Single crystals, grown by a hollow cathode plasma floating zone technique, using a pre-compacted

rod of high purity Cu_2O powder, were generously supplied through the Crystal Preparation Group (H. Parker) at the National Bureau of Standards (USA). Polycrystalline material was prepared using the method described by Toth *et al.* [5].

Compression specimens approximately 4 mm high by 2 mm x 2 mm cross-section for mechanical testing were cut from the single and polycrystalline material by sawing with a diamond slitting saw blade.

In the case of the single crystals, two orientations were selected for the compression axis, ⟨0 5 1⟩ for the high pressure experiments and ⟨1 2 2⟩ for the high temperature deformation. Under ⟨0 5 1⟩ axis the maximum resolved shear stress is applied to the $\{1\,\bar{1}\,0\}\langle 1\,1\,1\rangle$ and $\{1\,\bar{1}\,0\}\langle 1\,1\,0\rangle$ systems. Although the $\{1\,\bar{1}\,0\}\langle 1\,1\,1\rangle$ system was not found to be active in [1] and [6] it corresponds to the most closely placed planes and directions and hence might be expected to be the operative slip system. Under the ⟨1 2 2⟩ axis the same resolved shear stress is applied to the $\{1\,0\,1\}\langle 0\,1\,0\rangle$ and $\{0\,1\,0\}\langle 1\,0\,1\rangle$ systems simultaneously.

The specimens were oriented before and after cutting with the Laue back reflection X-ray method. After sawing, the faces of the specimens were polished one by one on 3/0 emery polishing paper using a steel holder. The holder consisted of a large steel flange with a hole perpendicular to the flange base. The specimen is mounted with crystal bond on one of the faces of a brass cylinder. This cylinder is fitted on the centre hole of the steel flange. The large surface area of the flange prevents tipping of the specimen during hand polishing.

Before mechanical testing, the specimens were chemically polished at room temperature in a mixture of 50% orthophosphoric acid and 50% nitric acid.

The specimens to be tested at high temperature were covered with an evaporated thin film of gold ($\simeq$ 100 Å) in order to prevent oxidation of the specimen. In this way it was possible to observe the slip lines of the surface of the specimen after testing at high temperatures.

2.2. Thin foil preparation

Foils for transmission electron microscopy were prepared by cutting thin slices (0.5 mm) with a diamond saw from compression specimens before and after testing. The slices were mechanically polished to 0.3 mm and then discs 3 mm diameter were cut with an ultrasonic drill. These discs were polished chemically by directing a gravity jet of 20% nitric acid in orthophosphoric acid at room temperature, until the central portion become a yellow colour indicating a thickness of about 1000 Å [8]. Thinning was continued either by ion bombardment (6 keV, Ar ions), or chemically by immersion in a bath of 60% orthophosphoric acid and 10% nitric acid for several minutes until a hole was perforated.

2.3. Apparatus and procedures

The high pressure apparatus used in this study, which has been described elsewhere [9], is essentially a constant cross-head speed tensile machine contained within a pressure chamber filled with a pressure-transmitting fluid. The tensile load applied to the specimen was measured by a pressure-compensating load cell within the pressure chamber. Strain was monitored from the "cross-head travel" at the movable end of the specimen by means of a linear transducer. The pressure fluid was a solution of 10% methyl alcohol in castor oil. The compression assembly is capable of operating at pressures up to 15 kb. All experiments were conducted at constant pressure and constant cross-head speed of 0.1 mm min^{-1}.

The high temperature and one atmosphere compression tests were performed in an Instron machine at a cross-head speed of 0.01 mm min^{-1}. During the deformation, the specimens were heated by an image type furnace. The tests were done from room temperature to 600° C.

3. Results

3.1. Stress and strain behaviour

Fig. 1 shows the typical stress–strain curves of single crystals and polycrystalline specimens of cuprous oxide, at various pressures. No plastic deformation was detected in the region from atmospheric pressure to 4 kb. In this region, all specimens, both single and polycrystals, broke without yielding and no slip lines were observed in the recovered pieces. However, the fracture stress is seen to increase with the pressure. At 6 kb, plastic yielding occurs in single crystals at 27 kg mm^{-2}, followed by up to 1% strain before fracture. Slip markings are observed but many cracks are also present in the fractured specimens. At 8 kb and above, the ductility is increased significantly; the single crystals with compression

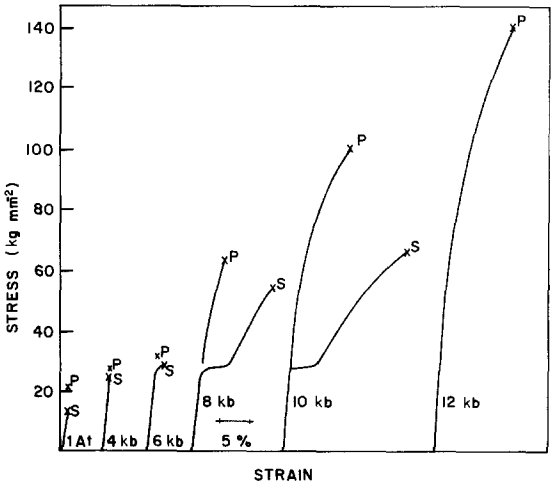

Figure 1 Effect of increased environmental pressure on the engineering stress–strain curve in compression – for Cu_2O single crystals (S) and polycrystals (P) (1 kb = 10 kg mm^{-2}).

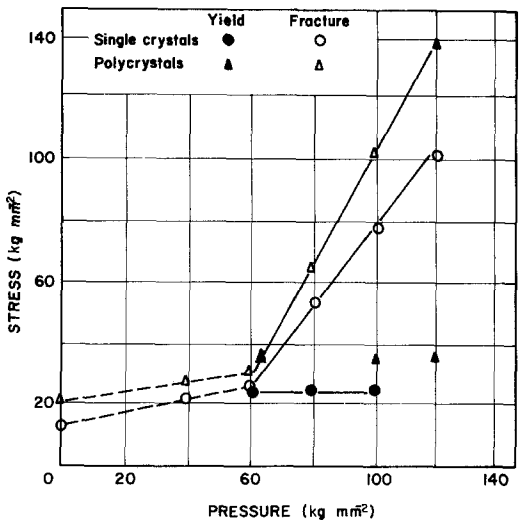

Figure 2 Pressure dependence of yield stress and fracture stress for Cu_2O single and polycrystals. (1 kb = 10 kg mm^{-2}).

axis ⟨0 5 1⟩ work-harden after a relatively large region of easy glide and reach a strain of some 15% before fracture. The polycrystals show a flow curve with rapid rates of strain hardening and extensive plastic deformation. Although crack propagation is thus suppressed by pressure in Cu_2O, the nucleation of cracks seemed to occur at all pressures studied here.

The transition temperature and stress–strain behaviour in the high temperature and one atmosphere deformation experiments were essentially the same as those obtained by [1] and [6] and will not be reproduced here.

3.2. High pressure effects

Fig. 2 summarizes the pressure dependence of the yield and fracture stresses. It is observed that the suppression of fracture i.e. increase in fracture stress, shows up as a discontinuity in the pressure dependence of fracture stress at about 6 kb. After this discontinuity, the pressure starts to be more effective in the suppression of fracture. The cleavage fracture theory of Francois and Wilshaw [10] predicts qualitatively a transition in the controlling fracture stage, similar to the one observed here. Another observation we can make from Fig. 2 is that the yield behaviour of Cu_2O single crystals and polycrystals is essentially unaffected by pressures up to at least 12 kb. This means that no appreciable changes occur in the structure of Cu_2O (phase transformation) when it is subjected to less than 12 kb.

3.3. Determination of glide elements

The main operative glide planes were of the {1 1 0} and {1 0 0} type for the ⟨1 2 2⟩ compression axis (tested at high temperature) and {1 1 0} type for the ⟨0 5 1⟩ compression axis (tested at high pressure). This identification was made by slip trace analysis on two adjacent perpendicular surfaces of single crystal specimens, and it is in agreement with the glide planes reported by [1], [6] and [7].

Thin foils were prepared from undeformed specimens and from specimens deformed at 8, 10 kb and at 500° C (one atmosphere) at different levels of strain. Thin foils from non-deformed

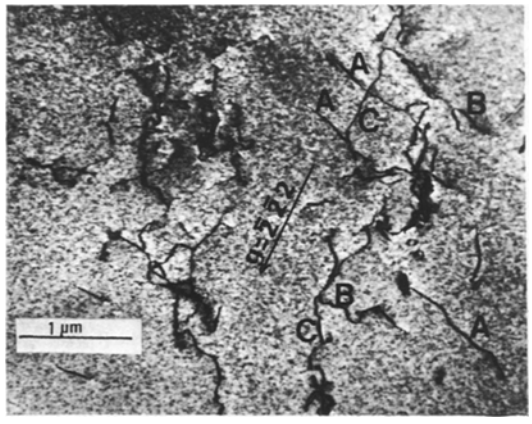

Figure 3 Dislocations in Cu_2O single crystal, deformed 4% at 500° C compression axis ⟨2 1 2⟩. The Burgers' vectors were ⟨1 0 1⟩ for dislocations A, ⟨0 1 0⟩ for B and ⟨$\bar{1}$ 1 1⟩ for C (200 kV).

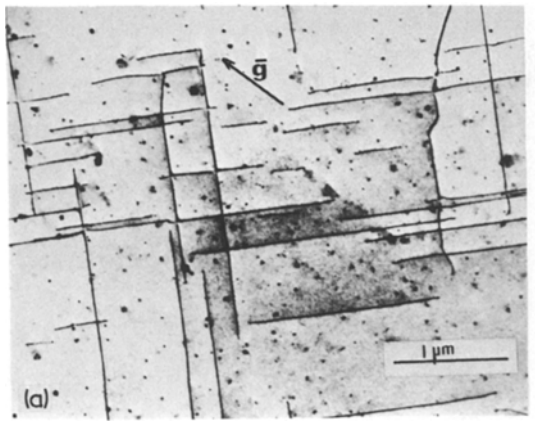

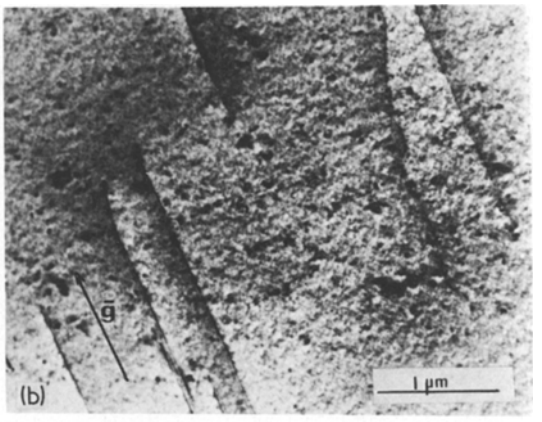

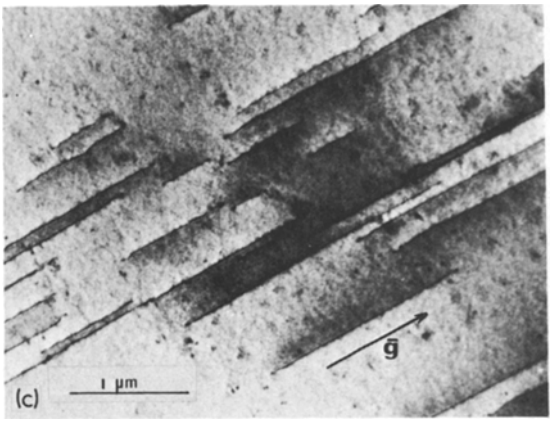

Figure 4 (a) Network of ⟨1 0 0⟩ and ⟨0 1 0⟩ dislocations in polycrystalline Cu_2O deformed 4% at 500° C. (b) **g** = 2 0 0. (c) **g** = 0 2 0.

specimens showed a very low dislocation density. After deformation the specimens showed several dislocation arrangements; dislocation loops, dislocation dipoles, elongated loops, etc. No difference in the dislocation structures was found when the specimens were deformed at high pressures at room temperature or high temperatures at one atmosphere.

Diffraction constrast experiments showed that the dislocations had Burgers vectors of the type ⟨1 1 1⟩, ⟨1 1 0⟩ and ⟨1 0 0⟩. This result is illustrated in Fig. 3, which shows a foil obtained from a single crystal deformed 4% with compression axis ⟨2 1 2⟩ at 500° C. The experiments show that dislocations such as "A" having Burgers vector ⟨1 0 1⟩ are out of contrast under ⟨0 2 0⟩ or ⟨$\bar{2}$ 0 2⟩. Dislocations "B" are out of contrast for ⟨2 0 $\bar{2}$⟩ and ⟨2 0 2⟩ reflections and have ⟨0 1 0⟩ Burgers vector, and dislocations "C" are invisible for ⟨2 2 0⟩ and ⟨0 2 $\bar{2}$⟩ reflections and have ⟨$\bar{1}$ 1 1⟩ Burgers vector. Fig. 4 shows a network of dislocations with {1 0 0} and {0 1 0} Burgers vectors, observed in a polycrystalline specimen deformed at 500° C. In the single crystals with compression axis ⟨0 5 1⟩ tested under high pressure, most of the observed dislocations were of the type ⟨1 1 1⟩. Dislocations with **b** of the ⟨1 0 0⟩ type were not observed because the resolved shear stress was too low to activate them. These dislocations observed in foils deformed 1% with compression axis ⟨0 5 1⟩ at 8 kb are out of contrast under ⟨$\bar{2}$ 4 $\bar{2}$⟩ and ⟨$\bar{2}$ 2 0⟩ reflections (Fig. 5). In Cu_2O, the apparent Burgers vector ⟨1 1 1⟩ is not the shortest lattice vector. To explain this observation, it is proposed that the dislocations gliding on the {1 $\bar{1}$ 0} ⟨1 1 1⟩ system are pairs of dislocations with a Burgers vector of the $\frac{1}{2}$ ⟨1 1 1⟩ type. The structure between the half dislocations is faulted only with respect to the Cu atoms; the oxygen atoms occupy normal anion sites. Some pairs of {1 1 1} dislocations are shown in Figs. 5 and 6.

4. Discussion

4.1. Effect of pressure on plastic deformation of Cu_2O

From the results of Figs. 1 and 4, we can observe that the principal effect of hydrostatic pressure on the mechanical behaviour of Cu_2O is to raise the stress at which fracture of the material will occur. Close to 6 kb, the deformation is elastic within the accuracy available. Optical observations of the recovered pieces do not reveal any slip markings. In this region between one atmosphere and 6 kb, the slope of the curve fracture stress versus pressure (Fig. 2) is less than one, i.e. an increase of pressure corresponds to a smaller increase in fracture

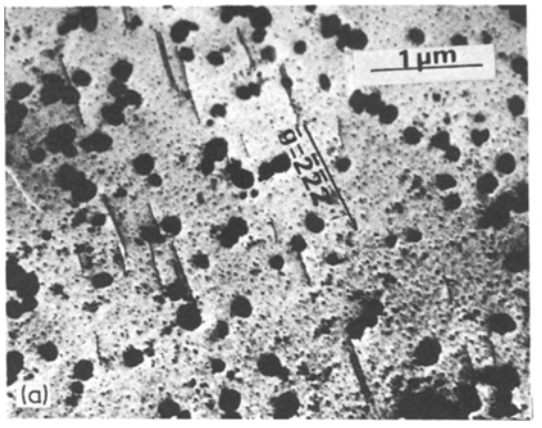

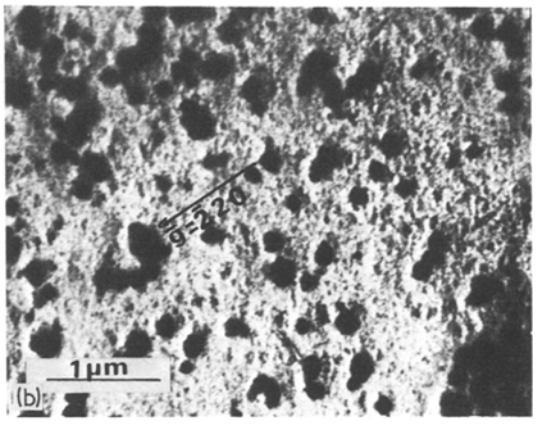

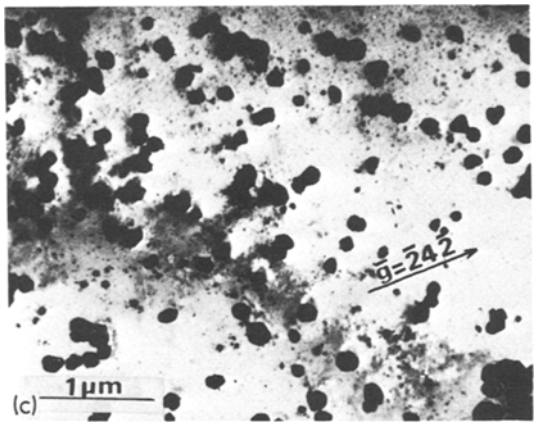

Figure 5 Diffraction contrast experiment in a specimen deformed 1% at 8 kb. The dislocations have Burgers' vectors ⟨1 1 1⟩. The black spots appeared after a long exposure time to the electron beam. Notice that some dislocations are pairs of dislocations (200 kV).

strength. This implies a weak effect of the pressure in controlling the propagation of the cracks. This propagation may occur in a Griffith manner in this region. In the region of the 6 kb, a brittle-to-ductile transition starts to occur and after 6 kb the slope of the curve changes from less than one to more than one, i.e. an increase in pressure corresponds to a greater increase in fracture strength. This change in the slope of the fracture strength versus pressure curve is predicted by the fracture theory of Francois and Wilshaw [9]. The slope of the fracture versus pressure curve after the transition point, according to the theory should be equal to one, the experimental curve showing a slope larger than one.

The reasons for the poor fit of the theory could be the following. Firstly, the only crack nucleation mechanism taken into account in the Francois and Wilshaw theory is the cleavage crack and it is assumed that the cracks are originated by dislocations pile-ups. In the present case, the latter mechanism is not a possible source of cracks because the cracks were observed to nucleate and propagate when the crystal was strained in the elastic region, i.e. when the mobility and number of dislocations is too low to produce pile-ups. Also, the sources of cracks in Cu_2O could be surface imperfections.

4.2. Slip direction in Cu_2O

The electron diffraction constrast experiments showed that the dislocations in deformed cuprous oxide, had ⟨1 1 1⟩, ⟨1 1 0⟩ and ⟨1 0 0⟩ type Burgers vectors. The crystallographic structure shows that the shortest distance for structural identity is *a* ⟨1 0 0⟩. To produce slip along ⟨1 1 1⟩, the dislocation of *a* ⟨1 1 1⟩ type must first dissociate

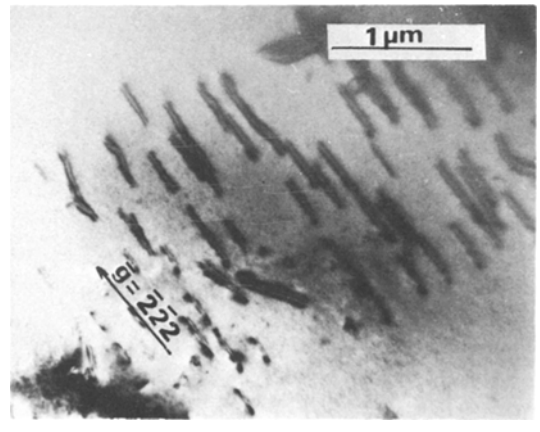

Figure 6 Extended dislocations of the ⟨1 1 1⟩ type observed in Cu_2O single crystals, deformed 0.5% at 8 kb. Compression axis was ⟨0 5 1⟩ (100 kV).

into partial dislocations with collinear Burgers vectors in $(1\,\bar{1}\,0)$ planes. Thus:

$$a\langle 1\,1\,1\rangle \rightarrow \frac{a}{2}\langle 1\,1\,1\rangle + \frac{a}{2}\langle 1\,1\,1\rangle$$

This dislocation reaction is encouraged by the reduction in elastic energy which accompanies it. In the limiting case where no Cu interstitial atoms exist, the $a/2$ $\langle 1\,1\,1\rangle$ dislocations are simply perfect dislocations in the b c c lattice of oxygen atoms.

In the Cu_2O structure, however, these two imperfect dislocations are partials, linked by a ribbon of copper stacking faults.

Suppose for the moment that they do not dissociate into perfect dislocations. Then as Nabarro [11] first pointed out, they can be expected to produce slip along $\langle 1\,0\,0\rangle$, as was observed, when the compression axis was $\langle 1\,2\,2\rangle$. This could be because the following dissociate into perfect dislocations:

$$a\langle 1\,1\,1\rangle \rightarrow a\langle 1\,0\,1\rangle + a\langle 0\,1\,0\rangle$$

$$a\langle 1\,0\,1\rangle \rightarrow a\langle 1\,0\,0\rangle + a\langle 0\,0\,1\rangle$$

involving no change of elastic energy, so that a stress that acts more strongly on one component, e.g. $a\langle 0\,1\,0\rangle$ of an $a\langle 1\,1\,1\rangle$ or $a\langle 1\,0\,0\rangle$ of an $a\langle 1\,0\,1\rangle$ dislocation, can move this component independently of the others.

4.3. Slip planes in Cu_2O

The choice of $\{1\,1\,0\}$ and $\{1\,0\,0\}$ planes for slip must mean that dislocations can move more easily on these planes then on any other plane. The $(1\,1\,0)$ type planes are the most densely packed with atoms and contain the slip directions $\langle 1\,1\,1\rangle$, $\langle 1\,1\,0\rangle$ and $\langle 1\,0\,0\rangle$. The approach of two copper ions during the slip in the $\langle 1\,1\,1\rangle$ and $\langle 1\,1\,0\rangle$ directions, does not seem to be very important in this structure that is more covalent than ionic [12].

The fact that the dislocations with Burgers vector $a\langle 1\,1\,1\rangle$ are glide dislocations, makes possible the activation of the $\{2\,\bar{1}\,\bar{1}\}$ planes because they contain the slip direction $\langle 1\,1\,1\rangle$, as was observed in [7].

The association of pairs of half-dislocations in this structure could result from a lowering of the Pierls–Nabarro stress opposing dislocation motion and this favours the operation of $(1\,1\,0)$ slip planes.

5. Conclusions

The stress–strain behaviour under compression at constant strain rate of single and polycrystalline cuprous oxide and the associated microstructural changes have been studied as a function of environmental hydrostatic pressure at room temperature up to 12 kb and as a function of temperature and one atmosphere up to 600° C. It is apparent from the above discussion that:

(1) Plastic deformation in Cu_2O single crystals and polycrystals can be induced at room temperature. The necessary critical pressure is in the region of 6 kb.

(2) The fracture stress and strain are increased with increasing pressure for both single and polycrystals. The rate of increase shows a marked discontinuity at a critical pressure (i.e. a pressure-induced brittle-to-ductile transition) of some 6 kb.

(3) An optical study of the slip lines on oriented single crystals, deformed in compression under conditions of high temperature or high pressure and by electron diffraction constrast experiments, show that plastic deformation takes place as a result of slip on the $\{1\,\bar{1}\,0\}\langle 1\,1\,1\rangle$ system when the stress was applied in the $\langle 0\,5\,1\rangle$ direction and on the $\{1\,0\,1\}\langle 0\,1\,0\rangle$ and $\{\bar{1}\,0\,1\}\langle 1\,0\,1\rangle$ systems when the stress was applied in the $\langle 1\,2\,2\rangle$ directions.

(4) It is considered that slip in $\langle 1\,1\,1\rangle$ directions proceeds by movement of pairs of collinear half-dislocations with Burgers vector $\frac{1}{2}\langle 1\,1\,1\rangle$ type joined by an area of stacking fault. Structurally, the stacking faults are similar to antiphase boundaries, with the oxygen lattice approximately continuous across the boundary but with the copper atoms stacking being out of place.

Acknowledgements

This work has been supported in part by the International Copper Research Association.

References.

1. G. VAGNARD and J. WASHBURN, *J. Amer. Ceram. Soc.* **51** (1968) 88.
2. A.F. WELLS, "Structural Inorganic Chemistry" (Oxford, 1962).
3. H.W. SWANSON and R.K. FUGAT, "Standard X-Ray Diffraction Powder Patterns", Vol. II (National Bureau of Standards, USA), Cire No. 539 **23** (1953).
4. R.E. TYLECOTE, *J. Inst. Metals* 78 (1950) 301
5. R.S. TOTH, R. KILKSON and D. TRIVICH, *J. Appl. Phys.* **31** (1960) 1117.

6. M. MARTÍNEZ CLEMENTE, T. BRETHEAU and J. CASTAING, *J. Physique* **37** (1976) 895.
7. G. TORRES VILLASEÑOR, Ph.D Thesis, Case Western Reserve University, Cleveland (1972).
8. O. KUBASCHEWSKI and B.E. HOPKINS, "Oxidation of Metals and Alloys" 2nd edn. (Butterworths, London, 1962).
9. G. DAS and S.V. RADCLIFFE, *J. Japan. Inst. Metals* **9** (1968) 344.
10. D. FRANCOIS and T.R. WILSHAW, *J. Appl. Phys.* **39** (1968) 4170.
11. R.F.N. NABARRO, "Advances in Physics" **1** (1952) 269.
12. L. PAULING, "The Nature of the Chemical Bond" (Cornell University Press, Ithaca, New York, 1960) p. 254.

Received 28 November 1977 and accepted 17 February 1978.